UC Riverside
UC Riverside Previously Published Works

Title
Estimation of the dose of electronic cigarette chemicals deposited in human airways through passive vaping

Permalink
https://escholarship.org/uc/item/9nz8d4sg

Journal
Journal of Exposure Science & Environmental Epidemiology, 31(6)

ISSN
1559-0631

Authors
Su, Wei-Chung
Lin, Ying-Hsuan
Wong, Su-Wei
et al.

Publication Date
2021-11-01

DOI
10.1038/s41370-021-00362-0

Peer reviewed

Estimation of the Dose of Electronic Cigarette Chemicals Deposited in Human Airways through Passive Vaping

Wei-Chung Su[1,*], **Ying-Hsuan Lin**[2,3], **Su-Wei Wong**[4], **Jin Y. Chen**[3], **Jinho Lee**[1], **Anne Buu**[4]

[1]Department of Epidemiology, Human Genetics and Environmental Sciences, School of Public Health, University of Texas Health Science Center at Houston, Houston, Texas, USA

[2]Department of Environmental Sciences, University of California, Riverside, California, USA

[3]Environmental Toxicology Graduate Program, University of California, Riverside, California, USA

[4]Department of Health Promotion & Behavioral Sciences, School of Public Health, University of Texas Health Science Center at Houston, Houston, Texas, USA

Abstract

Background—Existing studies on the health effects of e-cigarettes focused on e-cigarette users themselves. To study the corresponding effects on passive vapers, it is crucial to quantify e-cigarette chemicals deposited in their airways.

Objective—This study proposed an innovative approach to estimate the deposited dose of e-cigarette chemicals in the passive vapers' airways. The effect of the distance between active and passive vapers on the deposited dose was also examined.

Methods—The chemical constituent analysis was conducted to detect Nicotine and flavoring agents in e-cigarette aerosol. The Mobile Aerosol Lung Deposition Apparatus (MALDA) was employed to conduct aerosol respiratory deposition experiments in real-life settings to generate real-time data.

Results—For e-cigarette aerosol in the ultrafine particle regime, the deposited doses in the alveolar region were on average 3.2 times higher than those in the head-to-TB airways, and the deposited dose in the passive vaper's airways increased when being closer to the active vaper.

Significance—With prolonged exposure and close proximity to active vapers, passive vapers may be at risk for potential health effects of harmful e-cigarette chemicals. The methodology developed in this study has laid the groundwork for future research on exposure assessment and health risk analysis for passive vaping.

Keywords

E-cigarette; Aerosol; Human airways; Respiratory deposition; Deposited dose

*Corresponding author: Wei-Chung Su, Wei-Chung.Su@uth.tmc.edu, *Address*: School of Public Health, University of Texas Health Science Center at Houston, 1200 Pressler Street., Suite W634, Houston, TX 77030, *Tel*: 713-500-9762; *Fax*: 713-500-9750.

Introduction

Although electronic cigarettes (e-cigarettes) do not produce carcinogenic ashes and tar in e-cigarette aerosol, research has shown that inhalation of Nicotine through vaping is associated with negative health outcomes including heart rate change, blood pressure change, reduced FEV_1 and FVC, and vaping tongue [1–4], not to mention the risk for addiction. Furthermore, as a strategy to attract young consumers, e-cigarette companies add flavoring chemicals that are aerosolized together with Nicotine during vaping and then inhaled into human airways [5, 6], resulting in negative health consequences such as coughing, shortness of breath, wheezing, headache, fever, lung problems, and heart diseases [7–11]. These health effects of e-cigarettes were mainly found by previous research on e-cigarette users themselves (i.e., active vapers). Although it is reasonable to expect that similar effects may be applied to passive vapers based on the second-hand smoking literature, existing research on passive vaping is very limited. In fact, passive vapers could also be at risk for negative health effects because they tend to inhale smaller, aged, and chemical-enriched e-cigarette aerosol that is likely to enter into lower human airways. This is due to the natural process of diffusion and evaporation that E-cigarette aerosol is expected to reduce in size after traveling a distance in the air. Therefore, e-cigarette chemical constituents with low volatility or low vapor pressure tend to be enriched in such aged e-cigarette aerosol. This study focuses on quantifying e-cigarette chemicals deposited in passive vapers' airways, which is a crucial step to understand the health effects of passive vaping.

E-cigarette aerosol generated from vaping is a mix of liquid droplets. It is reported that the mode of e-cigarette aerosol size in the indoor environment is smaller than 50 nm [12–14]. With such a range of particle diameters, a great amount of inhaled e-cigarette aerosol is expected to enter and deposit in the deep lung, causing a considerable deposited dose because of the enormous airway surface area in the alveolar region. The deposited dose is the antecedent of the internal dose before considering respiratory clearance and absorption rate. Thus, the deposited dose of e-cigarette aerosol may serve as an optimal index of health risk assessment for passive vaping. The key step for accurately estimating the deposited dose is to obtain high-quality data of e-cigarette aerosol respiratory deposition. Yet, due to the limitations of conventional experimental methods, existing studies have relied on a partial human airway replica or numerical simulations [15, 16].

To deal with these critical limitations, our team recently developed an innovative experimental method, the Mobile Aerosol Lung Deposition Apparatus (MALDA), that consists of a set of representative human airway replicas and a pair of ultrafine particle (UFP) spectrometers to estimate the respiratory deposition of UFPs in the entire human airways, with the special feature of being transportable between laboratories and real-life settings. Unlike traditional methods, the MALDA can generate real-time deposition data and thus is highly efficient and practical. Further, the capacity of MALDA for estimating the respiratory deposition associated with passive vaping has been validated in the laboratory as well as in an indoor real-life setting [17].

In this study, we further apply the MALDA to fill important knowledge gaps in the literature. First, existing chemical analysis has been conducted using e-liquid that does not necessarily reflect the chemicals actually deposited in human airways [9]. Therefore, in this study, we conduct chemical analyses based on e-cigarette aerosol instead. Our chemical analysis also focuses on a selected set of e-cigarette chemicals that have been classified as irritants such as δ-Dodecalactone and Menthol [9], or proven to cause adverse health effects such as Benzyl Alcohol and Corylone [18–21]. Second, we propose a new approach to estimate the dose of e-cigarette chemicals in human airways by integrating the respiratory deposition estimated by MALDA with the chemical analysis results. This will allow nicotine and tobacco researchers to understand not only *what* chemical but also *how much* of the chemical is deposited in a passive vaper's respiratory system. Third, we examine whether the deposited dose is affected by the distance between active and passive vapers. Given that this is an important research question with policy implications and yet has not been investigated, our result will have a significant contribution to public health.

Method

Mobile aerosol lung deposition apparatus (MALDA)

The MALDA used in this study contains (1) a realistic human airway system from the oral cavity, larynx, tracheobronchial (TB) airways with 11th lung generation, down to a representative alveolar region; and (2) a UFP measurement system that consists of two units of scanning mobility particle spectrometers (SMPS+C, GRIMM Aerosol Technology, Ainring, Germany), which can capture the UFP size distributions at the inlet and outlet simultaneously to estimate the respiratory deposition (i.e., the inlet-outlet difference). The MALDA was made moveable by placing these two systems on a lab cart with an oil-free vacuum pump. Fig. 1 shows the schematic diagram of the MALDA used in this study. With such an advanced design, the MALDA is able to characterize the respiratory deposition of UFPs in not only the head-to-TB airways but also the alveolar region under an inspiratory flow rate of 30 L/min. The performance evaluation tests of the MALDA showed that the deposition data obtained by MALDA agreed quite well with conventional aerosol respiratory deposition curves [22–24]. Details regarding the MALDA design, development, dimensions, laboratory tests, and applications can be seen in our previous publications [17, 24–26].

Measurement of e-cigarette aerosol respiratory deposition in a real-life setting

The e-cigarette aerosol respiratory deposition experiments of this study were conducted at a voluntary e-cigarette user's apartment where the total space of the living room plus the dining area was approximately 50 m³. The MALDA was deployed at 2 m and 4 m away from the e-cigarette user in the living room to simulate common passive vaping scenarios. Before each experiment, the air in the room was carefully kept clean and calm without any aerosol generation or agitation activities for 5 hours to eliminate potential undesired background particles. The experiment was started with measuring the aerosolize distribution in the background and followed by a vaping episode that the e-cigarette user vaped JUUL-Virginia Tobacco freely for 20 minutes with similar puffs during each event. The MALDA was operated at the 30 L/min inspiratory flow rate. E-cigarette aerosol entering into the MALDA was measured by the UFP sizer A connected at the head inlet of the MALDA,

whereas e-cigarette aerosol passing through the TB airways and the alveolar region was measured in turn by the UFP sizer B at the TB airways and the alveoli outlets. Three runs of measurement for the aerosol size distribution were conducted at each inlet and outlet (3 mins for each run; about 20 minutes for all measurements). A total of eight visits were made to the apartment performing the same experimental procedure. Each visit was dedicated to only one distance setting (2 m or 4 m) and the total experiment time was approximately 40 minutes including setting up and packing up.

Based on the e-cigarette aerosol size distributions measured at the inlet and two outlets on the MALDA, the deposition fractions of the e-cigarette aerosol in the head-to-TB airway and the alveolar region were calculated using the following equations:

$$D_{H+TB, d} = (1 - \frac{C_{TB, d}}{C_{H, d}}), \tag{1}$$

$$D_{Alv, d} = (1 - \frac{C_{Alv, d}}{C_{H, d}}) - (1 - \frac{C_{TB, d}}{C_{H, d}}), \tag{2}$$

where $D_{H+TB,d}$ and $D_{Alv,d}$ are the deposition fraction (0 to 1) of e-cigarette aerosol with size d nm in the head-to-TB airway and the alveolar region, respectively; and $C_{H,d}$, $C_{TB,d}$, and $C_{Alv,d}$ are the particle number concentrations (aerosol size distributions) measured at the head inlet, TB outlet, and alveoli outlet, respectively. Detailed explanations of these equations can be found in our previous publication [24].

E-cigarette aerosol chemical constituent analysis

To estimate the deposited dose of a specific e-cigarette chemical substance in the passive vaper's respiratory system, it is essential to acquire the information of size-dependent chemical constituents for e-cigarette aerosol. For this purpose, a chamber study was conducted in the laboratory to collect e-cigarette aerosol samples of JUUL-Virginia Tobacco that were later used in chemical analyses. Fig. 2 shows the schematic of the setup of the e-cigarette aerosol collection experiment. The chamber with the dimensions of 61 cm (L) × 61 cm (W) × 61 cm (H) was used in our previous MALDA study for 3D printing emission research [24]. An electric fan was installed inside the chamber to mix the e-cigarette aerosol well. A 30 ml syringe was used to draw e-cigarette aerosol from the JUUL device and pump e-cigarette aerosol into the chamber. The e-cigarette aerosol was then pulled from the chamber to a Micro-orifice Uniform Deposit Impactor (MOUDI 110-R, MSP Co., Shoreview, MN, USA) operated at the 30 L/min sampling flow rate to collect e-cigarette aerosol samples. This sample collection was mainly conducted on the last four stages of MOUDI (cut-off diameters: 56, 100, 180, and 320 nm) that captured the particle sizes associated with passive vaping; and the procedure lasted for 60 mins to accumulate a sufficient amount of e-cigarette aerosol for subsequent chemical analysis. E-cigarette aerosol was sampled onto PTFE membrane filters (PALL Co., Port Washington, NY, USA) which were placed on MOUDI stages. After the sample collection, PTFE filters with collected e-cigarette aerosol samples were immediately unloaded from the MOUDI, put in individual

glass vials, and shipped overnight with dry ice to a well-established wet lab for chemical analysis.

The chemical analysis was conducted using two different analytical techniques to gain the best sensitivity to detect Nicotine and flavoring agents in the e-cigarette aerosol, including (1) liquid chromatography coupled with diode array detection and electrospray ionization-quadruple-time of flight-mass spectrometry (LC-DAD/ESI-Q-TOF-MS, Agilent 6545), and (2) gas chromatography/electron ionization-mass spectrometry (GC/EI-MS, Agilent 6890N GC and 5975C MSD) with trimethylsilylation. The former instrument is optimized for Nicotine detection, whereas the latter one is ideal for detecting other oxygenated harmful chemicals in e-cigarette aerosol. Targeted analysis for known harmful and potentially harmful constituents present in e-liquids was performed with a specific focus on those toxic flavoring agents reported in the literature and the publicly accessible E-liquid database (https://eliquidinfo.org/) [27].

To identify and quantify Nicotine and selected flavoring agents, PTFE filters with deposited e-cigarette particles in different sizes were extracted with 10 mL of isopropyl alcohol (IPA) under 60 mins of sonication. After sonication, the solutions of filter extracts were transferred to a pre-cleaned scintillation vial and concentrated under a gentle stream of nitrogen. The recovery of target analytes was determined by spiking a known amount of chemicals onto blank filters. Spiked filers were extracted in the same manner as collected aerosol samples (the percent recovery from the spiked samples was around 70% on average). Each of the target analytes was quantified using authentic standards and normalized to the internal standard responses to account for the instrumental variability. For LC-DAD/ESI-Q-TOF-MS analysis, the dried residues were reconstituted with 150 μL of IPA and transferred into 2 mL amber vials with 200 μL deactivated glass inserts. An Agilent Poroshell 120 EC-C18 column (3.0×50 mm, 2.7 μm particle size) was used for chromatographic separations. 50 μL of each sample was injected onto the LC column and eluted with solvent mixtures of acetonitrile containing 0.1% formic and water containing 0.1% formic acid as mobile phases at a flow rate of 0.3 mL/min. The in-line DAD recorded the signal at 260 nm for nicotine detection (with a reference wavelength at 360 nm) and MS was operated in positive ion mode. For GC/EI-MS analysis, the dried residues were trimethylsilylated with 100 μL of N,O-bis(trimethylsilyl) trifluoroacetamide with trimethylchlorosilane (BSTFA + TMCS, 99 : 1) (99%, SUPELCO) and 50 μL anhydrous pyridine (99%, EMD Millipore Corporation) at 70 °C for 1 hour. This derivatization procedure allows the conversion of oxygenated flavor chemicals (e.g., alcohols, phenols, and carboxylic acids) into volatile trimethylsilyl (TMS) derivatives. 5 μL of each sample was injected onto the GC column (Agilent J&W DB-5MS column, 30 m $\times$ 0.25 mm, 0.25 μm, i.d.) in splitless mode. Helium (ultra-high purity, 99.999%) was used as the carrier gas and set at a flow rate of 1 mL min^{-1}. The MS scan was performed within the *m/z* 30–400 range. The inlet/injector temperature was set at 250 °C. The MS transfer line temperature was 280 °C. The GC temperature program for analyses was: 40 °C hold for 1 min, 5 °C/min to 200 °C, and then 40 °C/min to 280 °C. The MS was operated in electron ionization mode at 70 eV. The ion source temperature was 230 °C, and the quadrupole temperature was 150 °C.

The purpose of the MOUDI chemical analysis approach is to estimate the chemical mass fraction for a range of e-cigarette aerosol sizes (The mass of a specific chemical to the total chemical mass collected on a MOUDI stage). The results of chemical mass fractions in different aerosol size ranges were later used for calculating the deposited dose.

Estimation of deposited dose for e-cigarette chemicals

Define $DD_{k,i,d}$ as the hourly deposited dose (μg/hr) of an e-cigarette chemical k in the human airway section i caused by the deposition of an e-cigarette particle with a diameter d in that airway section. Based on inhalation toxicology, $DD_{k,i,d}$ can be calculated by the following equation:

$$DD_{k,i,d} = D_{i,d} \times M_d \times C_{k,d} \times V,$$ (3)

where $D_{i,d}$ is the aerosol respiratory deposition fraction (0 to 1) in the human airway section i (H+TB: head-to-TB airways; Alv: alveolar region) for an e-cigarette particle with a diameter d; M_d is the mass concentration (μg/m^3) of e-cigarette aerosol with a diameter d inhaled into the human airways; $C_{k,d}$ is the mass fraction (0 to 1) of a specific chemical substance k in the e-cigarette particle with a diameter d; V is the total air volume inhaled by a normal person per hour (m^3/hr). To estimate $DD_{k,i,d}$ in this study, $D_{i,d}$ was acquired by MALDA using Eq. (1) and Eq. (2); M_d was converted from number concentrations obtained by the UFP sizer A on the MALDA. The density of Glycerol (1.26 g/cm^3) was used for converting number concentrations to mass concentrations since Glycerolis has a high boiling point and is one of the base constituents of e-liquids; $C_{k,d}$ was derived from the laboratory chemical analysis; V was set to be 0.6 m^3/hr based on the data of adult minute ventilation under low activities with a breathing frequency of 13/min and tidal volume of 0.77 L [28]. Given all the above values, the hourly deposited dose ($DD_{k,i,d}$) of a specific e-cigarette chemical substance in the head-to-TB airways, the alveolar region, and the entire human respiratory tract can be properly estimated by using Eq. (3).

Results

Table 1 depicts the chemical constituents of e-cigarette aerosol obtained from the chemical analysis. Data shown in the table are mass fractions of major chemical substances and selected flavoring agents in the e-cigarette aerosol. The size-dependent chemical analysis was based on the cut-off diameter of the MOUDI stage. The result indicates that the passive vaping related e-cigarette aerosol generated by JUUL-Virginia Tobacco contains high concentrations of Glycerol, δ-Dodecalactone, and Nicotine. The mass fractions of chemicals in the e-cigarette aerosol showed a function of the particle size and were also affected by the physical property of the chemical. For instance, for chemicals with high boiling points (low vapor pressure) such as Triethyl Citrate, their mass fractions in the aerosol increased as the aerosol size decreased. In contrast, for chemicals with low boiling points (high vapor pressure) such as Propylene Glycol (PG), their fractions in the aerosol decreased as the aerosol size decreased due to the natural evaporation. As can be seen in Table 1, the amount of PG collected on the last three MOUDI stages (the small particle size range) was below the detection limit of the GC/MS. However, a certain amount of PG was

detected in the larger e-cigarette aerosol size range (320   d   560) and the associated mass fraction was found to be 0.0092.

Figs. 3a and 3b show the particle size distributions of the background aerosol (without vaping) and the e-cigarette aerosol measured at two distances (2 m and 4 m) in the real-life setting. The size distributions are shown in both number concentrations (Fig. 3a) and converted mass concentrations (Fig. 3b). As shown in Fig. 3a, from the viewpoint of particle number concentration, a considerable amount of passive vaping associated e-cigarette aerosol was in the regime of ultrafine particle (particle diameter < 100 nm), which is consistent with what were found in published studies that the mode of e-cigarette aerosol diameter in the environment was generally smaller than 50 nm [12–14]. In this study, the number concentration of e-cigarette aerosol was higher at 2 m than at 4 m. The t-test result showed that the number concentration across different particle sizes was significantly higher at 2 m compared to 4 m with t = 2.84, df = 74, p < 0.01. This result implies that the closer the passive vaper is to the active vaper, the more e-cigarette aerosol the passive vaper will inhale. The size of the e-cigarette aerosol was slightly larger at 2 m (peaked at 36 nm) than at 4 m (peaked at 30 nm). This may result from the evaporation of the liquid e-cigarette aerosol after traveling a distance in the air. On the other hand, the peaks of the corresponding mass concentration were around 110 to 120 nm for both distances (see Fig. 3b).

Figs. 3c and 3d show the deposition fractions of e-cigarette aerosol in the head-to-TB airway ($D_{H+TB,d}$) and the alveolar region ($DD_{Alv,d}$) obtained by the MALDA under two different measurement distances. The results as presented have undergone both the intra-instrument correction and the MALDA wall-loss correction (particle losses in the inner surfaces of the MALDA) as conducted in our previous research [24–25]. The deposition of e-cigarette aerosol in the head-to-TB airway at 2 m was slightly higher than that at 4 m, resulting in slightly lower aerosol deposition in the alveolar region at 2 m compared to that at 4 m. The deposition fractions in the head-to-TB airway were generally less than 40% and decreased as the particle size increased. Such a negative association between deposition fractions and particle sizes was even greater in the alveolar region. Deposition fractions in the alveolar region were high (about 60%) at around 15 nm. In general, the respiratory deposition fractions between the two measurement distances were similar, since the t-test results indicated that the deposition fractions across different particle sizes at 2 m were not significantly different from that at 4 m for both the head-to-TB airway (t = 0.22, df = 74, p > 0.1) and the alveolar region (t = 0.13, df = 74, p > 0.1).

Given the size-dependent chemical constituent (Table 1), the e-cigarette aerosol size distribution (Figs. 3a and 3b), and the respiratory deposition fractions (Figs. 3c and 3d), the deposited dose of a specific e-cigarette chemical in the human airways can then be properly estimated using Eq. (3) for passive vaping related e-cigarette aerosol measured in the ultrafine particle regime. Fig. 4 presents the deposited dose (per hour) for e-cigarette aerosol (Fig. 4a), Nicotine (Fig. 4b), and Benzyl Alcohol (Fig. 4c) in the head-to-TB airway and the alveolar region. The data of size-dependent chemical mass fractions listed in Table 1 were applied to corresponding e-cigarette aerosol with diameters within the collectible particle size range of a MOUDI stage. The data of the last MODUI stage was applied to

e-cigarette aerosol less than 56 nm. As shown in Fig. 4, the deposited doses in the alveolar region are relatively higher than those in the head-to-TB airways.

Fig. 5 shows the cumulative deposited dose of all particle diameters (10 to 130 nm) and all e-cigarette chemicals examined in this study. Overall, the cumulative deposited doses in the entire human airway were higher at 2 m than those at 4 m. This result is mainly due to the comparatively higher e-cigarette aerosol concentration at 2 m as shown in Fig. 3b. The Glycerol had the highest cumulative deposited dose in the passive vaper's airway, followed by δ-Dodecalactone (another flavoring agent) and then Nicotine. The cumulative deposited doses of other flavoring agents were generally less than 0.0008 μg/hr. The ratios of the deposited dose in the alveolar region to that in the head-to-TB airway for target chemicals were higher at 4 m (3.5 to 4.7) than the ratios at 2 m (2.8 to 3.0). These results are related to the finding that slightly more deposition was found in the alveolar region at 4 m than at 2 m. It is worth noting that the data shown in Fig. 5 are deposited doses *per hour*. As the exposure time increases, these numbers are expected to increase proportionally.

Discussion

The respiratory deposition of e-cigarette aerosol showed similar results at 2 m and 4 m (Figs. 3c and 3d) reflected the fact that the aerosol respiratory deposition fraction is primarily a function of the particle size [22, 23], and thus is basically unaffected by the particle concentration that differs across distances. The particle size measured by the SMPS in this study is the particle electrical mobility diameter. However, it has been reported that while the physical diameter of the aerosol is less than 100 nm such as the e-cigarette aerosol size measured in this study, the electrical mobility diameter is close to the aerodynamic diameter which is more often used in aerosol respiratory deposition [29].

Relatively more e-cigarette aerosol was found to deposit in the alveolar region. This result is expected because (1) the size range of the e-cigarette aerosol is in ultrafine particle regime; and (2) there is a tremendous total surface area in the human alveolar region, making the alveolar region the primary deposition and absorption site for inhaled e-cigarette aerosol. Therefore, the deposited dose in the alveolar region is an ideal index (compared to that in the head-to-TB airways) for quantifying the internal dose of e-cigarette chemicals in the passive vaper's lung. Indeed, our finding indicated that the deposited doses of e-cigarette chemicals in the alveolar region are on average 3.2 times higher than those in the head-to-TB airways for e-cigarette aerosol in the ultrafine particle regime.

Among the three chemicals with the highest cumulative deposited doses, the flavoring agent, δ-Dodecalactone, has been classified as an irritant [9]. Inhalation of Nicotine through vaping has also been shown to be associated with negative physical health outcomes including heart rate change [1], blood pressure change [2], reduced FEV_1 and FVC [3], and vaping tongue [4], as well as negative mental health outcomes such as addiction, change alertness, reduced appetite, impulse control, memory, learning and focusing problems, and ADHD symptoms [30–34]. Although the hourly cumulative deposited doses for those chemicals associated with adverse health effects such as Benzyl Alcohol and Corylone are low [18–21], passive vapers with prolonged exposure could still be subject to their negative impact. Future studies

that quantify the effects of cumulative deposited doses of these chemicals on short-term and long-term health outcomes may guide e-cigarette product regulations and indoor vaping policies.

From the point of view of inhalation toxicology, the deposited dose is predominantly determined by the mass concentration (large particles), but not the number concentration (small particles). Although the mass of e-cigarette aerosol was mainly contributed by e-cigarette aerosol larger than 100 nm (Fig. 3b), the particle number of e-cigarette aerosol around 100 nm was relatively small and approached the background (Fig. 3a). Our results showed that, within the e-cigarette size studied in this research (10 to 130 nm), the major contribution came from e-cigarette aerosol with the particle size ranging from 50 to 90 nm (Figs. 4b & 4c), which accounts for on average 54% of the total cumulative deposited dose. These results demonstrate that the MALDA could provide useful information to identify the critical size of e-cigarette aerosol within the size range studied (ultrafine particles) that contributes to the deposited dose found.

In this study, the deposited dose in the human respiratory tract was obtained by combining the MALDA experiments in the real-life setting and the MOUDI experiments in the laboratory. To implement the study, assumptions were made to integrate the two experiments, and limitations regarding the experimental methods used were also identified. For example, it was assumed that e-cigarette aerosols with the same particle diameters were having the same chemical fractions under similar temperature and humidity. In this way, the chemical mass fractions acquired from the laboratory MOUDI study could then be applied to e-cigarette aerosol measured by MALDA in the real-life setting for calculating associated deposited dose. Moreover, although the MALDA can acquire on-site aerosol respiratory deposition data, one limitation regarding the MALDA approach was found to be that the application of the MALDA is limited to ultrafine particles (particle diameter < 100 nm) according to its current features. Further improvements and upgrades will be needed on MALDA to enhance its overall function especially on estimating the respiratory deposition for aerosol with particle diameters larger than 100 nm. The improvement will include the installation of aerosol spectrometers that are capable of measuring particle size distribution across submicron to micron scale.

On the other hand, one of the potential limitations of the MOUDI approach on collecting e-cigarette aerosol samples is that a MOUDI stage collects a range of particle sizes but not one single particle size. Therefore, the mass fractions of individual chemicals were obtained as an average of all collectible particle sizes on that MOUDI stage. As a result, chemical mass fractions were discrete between adjacent MOUDI stages, which could cause unsmooth deposited doses as shown in Figs. 4b and 4c. Besides, the high pressure drop inside the MOUDI caused by the required flow rate could lead to possible losses of certain semivolatile chemicals in the e-cigarette aerosol. Therefore, errors are inevitably inherent in this MOUDI approach, and the chemical mass fractions obtained might not be precise. Nevertheless, the size-dependent chemical constituent obtained could still provide useful information as a reference on chemical mass fractions for e-cigarette aerosol in different particle size ranges.

Based on the results obtained from this study, the higher deposited dose estimated at 2 m (compared to 4 m) indicates that when the passive vaper is closer to the active vaper, more e-cigarette chemicals will be inhaled and deposited in the passive vaper's airway. To extend the current investigation on the effect of distances in secondary e-cigarette aerosol exposure, CFD (computational fluid dynamics) models will be employed in our future study to numerically simulate the e-cigarette aerosol concentration contour generated by active vapers in typical residential rooms or commercial areas. The simulated e-cigarette aerosol distribution together with the deposited dose estimated by the MALDA-approach should be able to provide evidence-based recommendations to policymakers and the general public regarding the minimum distance between active and passive vapers.

Conclusions

In this study, we developed an innovative approach, which integrates MALDA measurement of e-cigarette aerosol respiratory deposition with chemical constituent analysis on e-cigarette aerosol in the ultrafine particle regime, to estimate the deposited dose of targeted chemicals in a passive vaper's head-to-TB airways and alveolar region under two different distances (2 m and 4 m) from the active vaper. This approach built upon the unique strengths of the MALDA experimental approach, including transportability between laboratories and real-life settings, the full coverage of human airways, the capacity of generating real-time deposition data, and the specialty of capturing ultrafine particles that are abundant in e-cigarette aerosol. The results showed that a considerable number of passive vaping associated e-cigarette particles were in the ultrafine particle regime, and most of them deposited in the alveolar region and contributed to the deposited dose there. Therefore, with prolonged exposure and close proximity to active vapers, passive vapers may be at risk for potential health effects of harmful e-cigarette chemicals. In summary, this methodology development has laid the groundwork for future research on the health effects of passive vaping because one ought to be able to quantify what enters into a passive vaper's respiratory system before the effect of the dose on short-term or long-term health outcomes can be accurately assessed.

Funding

References

1. Hiler M, Breland A, Spindle T, Maloney S, Lipato T, Karaoghlanian N, et al. Electronic cigarette user plasma nicotine concentration, puff topography, heart rate, and subjective effects: Influence of liquid nicotine concentration and user experience. Exp Clin Psychopharmacol 2017;25(5):380–92. [PubMed: 29048187]

2. Dimitriadis K, Tsioufis C, Kontantinou K, Liatakis I, Andrikou E, Vogiatzakis N, et al. Acute detrimental effects of e-cigarette and tobacco cigarette smoking on blood pressure and sympathetic nerve activity in healthy subjects. Eur Heart J. 2019;40(Supplement_1):e245.

3. Kotoulas S-C, Pataka A, Domvri K, Spyratos D, Katsaounou P, Porpodis K, et al. Acute effects of e-cigarette vaping on pulmonary function and airway inflammation in healthy individuals and in patients with asthma. Respirology 2020;25(10):1037–45. [PubMed: 32239706]

4. Cho JH. The association between electronic-cigarette use and self-reported oral symptoms including cracked or broken teeth and tongue and/or inside-cheek pain among adolescents: A cross-sectional study. PLoS One. 2017;12(7):e0180506. [PubMed: 28700729]

5. Kosmider L, Sobczak A, Prokopowicz A, Kurek J, Zaciera M, Knysak J, et al. Cherry-flavoured electronic cigarettes expose users to the inhalation irritant, benzaldehyde. Thorax. 2016;71(4):376. [PubMed: 26822067]

6. Farsalinos KE, Kistler KA, Gillman G, Voudris V. Evaluation of Electronic Cigarette Liquids and Aerosol for the Presence of Selected Inhalation Toxins. Nicotine Tob Res 2014;17(2):168–74. [PubMed: 25180080]

7. Gerloff J, Sundar IK, Freter R, Sekera ER, Friedman AE, Robinson R, et al. Inflammatory Response and Barrier Dysfunction by Different e-Cigarette Flavoring Chemicals Identified by Gas Chromatography–Mass Spectrometry in e-Liquids and e-Vapors on Human Lung Epithelial Cells and Fibroblasts. Appl. In. Vitro Toxicol 2017;3(1):28–40.

8. Li Q, Zhan Y, Wang L, Leischow SJ, Zeng DD. Analysis of symptoms and their potential associations with e-liquids' components: a social media study. BMC Public Health. 2016;16(1):674. [PubMed: 27475060]

9. Omaiye EE, McWhirter KJ, Luo W, Pankow JF, Talbot P. High-Nicotine Electronic Cigarette Products: Toxicity of JUUL Fluids and Aerosols Correlates Strongly with Nicotine and Some Flavor Chemical Concentrations. Chem Res Toxicol 2019;32(6):1058–69. [PubMed: 30896936]

10. Muthumalage T, Lamb T, Friedman MR, Rahman I. E-cigarette flavored pods induce inflammation, epithelial barrier dysfunction, and DNA damage in lung epithelial cells and monocytes. Sci Rep 2019;9(1):19035. [PubMed: 31836726]

11. Anderson C, Majeste A, Hanus J, Wang S. E-Cigarette Aerosol Exposure Induces Reactive Oxygen Species, DNA Damage, and Cell Death in Vascular Endothelial Cells. Toxicol Sci 2016;154(2):332–40. [PubMed: 27613717]

12. Ji EH, Sun B, Zhao T, Shu S, Chang CH, Messadi D, et al. Characterization of Electronic Cigarette Aerosol and Its Induction of Oxidative Stress Response in Oral Keratinocytes. PLoS One. 2016;11(5):e0154447. [PubMed: 27223106]

13. Zhao T, Nguyen C, Lin C-H, Middlekauff HR, Peters K, Moheimani R, et al. Characteristics of secondhand electronic cigarette aerosols from active human use. Aerosol Sci Technol 2017;51(12):1368–76.

14. Zhang L, Lin Y, Zhu Y. Transport and Mitigation of Exhaled Electronic Cigarette Aerosols in a Multizone Indoor Environment. Aerosol Air Qual Res 2020;20(11):2536–47.

15. Zhou Y, Irshad H, Dye WW, Wu G, Tellez CS, Belinsky SA. Voltage and e-liquid composition affect nicotine deposition within the oral cavity and carbonyl formation. Tob Control 2020:tobaccocontrol-2020–055619.

16. Sosnowski TR, Kramek-Romanowska K. Predicted Deposition of E-Cigarette Aerosol in the Human Lungs. J. Aerosol Med Pulm Drug Deliv 2016;29(3):299–309. [PubMed: 26907696]

17. Su W-C, Wong S-W, Buu A. Deposition of E-cigarette aerosol in human airways through passive vaping. Indoor Air. 2021;31(2):348–56. [PubMed: 33020934]

18. Czoli CD, Goniewicz ML, Palumbo M, Leigh N, White CM, Hammond D. Identification of flavouring chemicals and potential toxicants in e-cigarette products in Ontario, Canada. Can J. Public Health 2019;110(5):542–50. [PubMed: 31025300]

19. Schober W, Szendrei K, Matzen W, Osiander-Fuchs H, Heitmann D, Schettgen T, et al. Use of electronic cigarettes (e-cigarettes) impairs indoor air quality and increases FeNO levels of e-cigarette consumers. Int. J. Hyg. Environ. Health 2014;217(6):628–37. [PubMed: 24373737]

20. Vardavas C, Girvalaki C, Vardavas A, Papadakis S, Tzatzarakis M, Behrakis P, et al. Respiratory irritants in e-cigarette refill liquids across nine European countries: a threat to respiratory health? Eur Respir J 2017;50(6):1701698. [PubMed: 29269582]

21. Farsalinos K, Lagoumintzis G. Toxicity classification of e-cigarette flavouring compounds based on European Union regulation: analysis of findings from a recent study. Harm Reduct J. 2019;16(1):48. [PubMed: 31345235]

22. ICRP. Human respiratory tract model for radiological protection. Publication 66. Annals of the ICRP. 1994;24:1–3.

23. Hinds WC. Aerosol Technology: Properties, Behavior, and Measurement of Airborne Particles: John Wiley & Sons; 1999.

24. Su W-C, Chen Y, Xi J. Estimation of the deposition of ultrafine 3D printing particles in human tracheobronchial airways. J. Aerosol Sci 2020;149:105605.

25. Su W-C, Chen Y, Bezerra M, Wang J. Respiratory deposition of ultrafine welding fume particles. J. Occup Environ Hyg 2019;16(10):694–706. [PubMed: 31461396]

26. Su W-C, Chen Y, Xi J. A new approach to estimate ultrafine particle respiratory deposition. Inhal Toxicol 2019;31(1):35–43. [PubMed: 30782028]

27. Sassano MF, Davis ES, Keating JE, Zorn BT, Kochar TK, Wolfgang MC, et al. Evaluation of e-liquid toxicity using an open-source high-throughput screening assay. PLoS Biol 2018;16(3):e2003904. [PubMed: 29584716]

28. Cuddihy R, Fisher G, Kanapilly G, Moss O, Phalen R, Schlesinger R, et al. Report No. 125—deposition, retention and dosimetry of inhaled radioactive substances. NCRP; 1997.

29. Hammer T, Gao H, Pan Z, Wang J. Relationship between aerosols exposure and lung deposition dose. Aerosol and Air Quality Research. 2020 5;20(5):1083–93.

30. Higgins ST, Heil SH, Sigmon SC, Tidey JW, Gaalema DE, Hughes JR, et al. Addiction Potential of Cigarettes With Reduced Nicotine Content in Populations With Psychiatric Disorders and Other Vulnerabilities to Tobacco Addiction. JAMA Psychiatry. 2017;74(10):1056–64. [PubMed: 28832876]

31. Jung Y, Hsieh LS, Lee AM, Zhou Z, Coman D, Heath CJ, et al. An epigenetic mechanism mediates developmental nicotine effects on neuronal structure and behavior. Nat Neurosci 2016;19(7):905–14. [PubMed: 27239938]

32. Jessen A, Buemann B, Toubro S, Skovgaard IM, Astrup A. The appetite-suppressant effect of nicotine is enhanced by caffeine. Diabetes Obes Metab 2005;7(4):327–33. [PubMed: 15955118]

33. Leach PT, Cordero KA, Gould TJ. The effects of acute nicotine, chronic nicotine, and withdrawal from chronic nicotine on performance of a cued appetitive response. Behav Neurosci 2013;127(2):303–10. [PubMed: 23565938]

34. Wilens TE, Decker MW. Neuronal nicotinic receptor agonists for the treatment of attention-deficit/hyperactivity disorder: Focus on cognition. Biochem Pharmacol 2007;74(8):1212–23. [PubMed: 17689498]
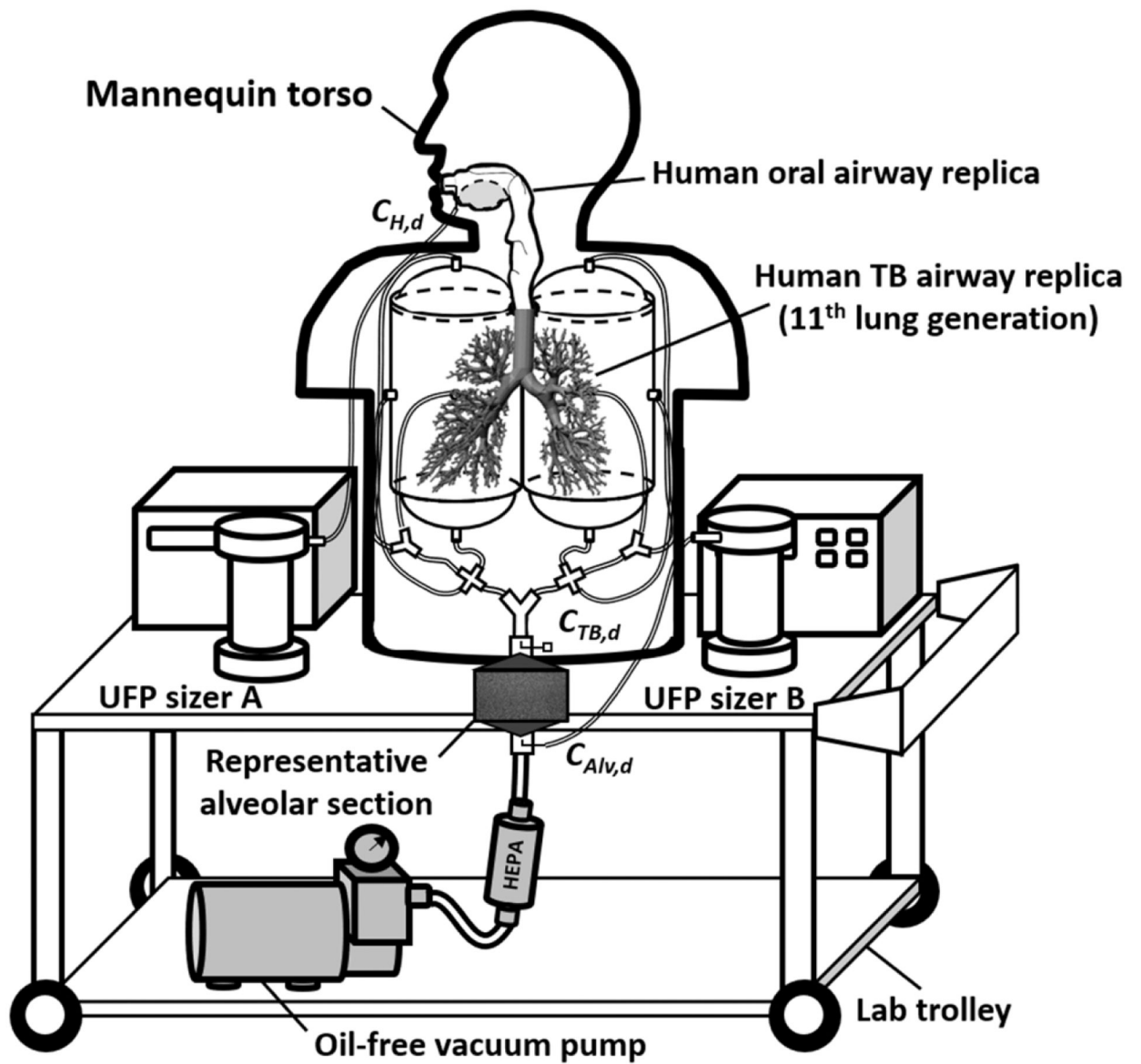
Fig. 1.
The schematic diagram of the Mobile Aerosol Lung Deposition Apparatus (MALDA).
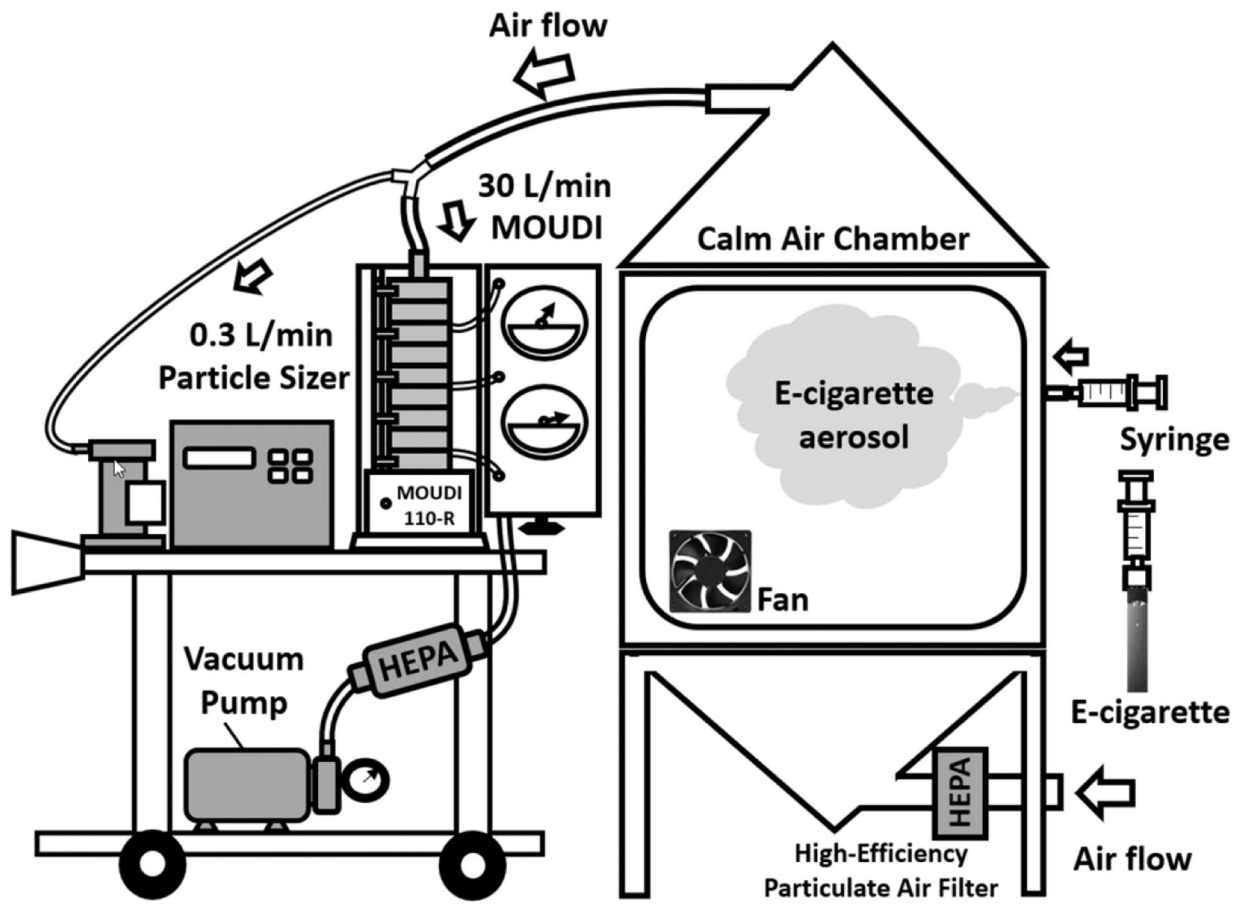
Air flow

Calm Air Chamber

30 L/min
MOUDI

0.3 L/min
Particle Sizer

E-cigarette
aerosol

Syringe

MOUDI
110-R

Fan

Vacuum
Pump

HEPA

E-cigarette

HEPA

High-Efficiency
Particulate Air Filter

Air flow

Fig. 2.
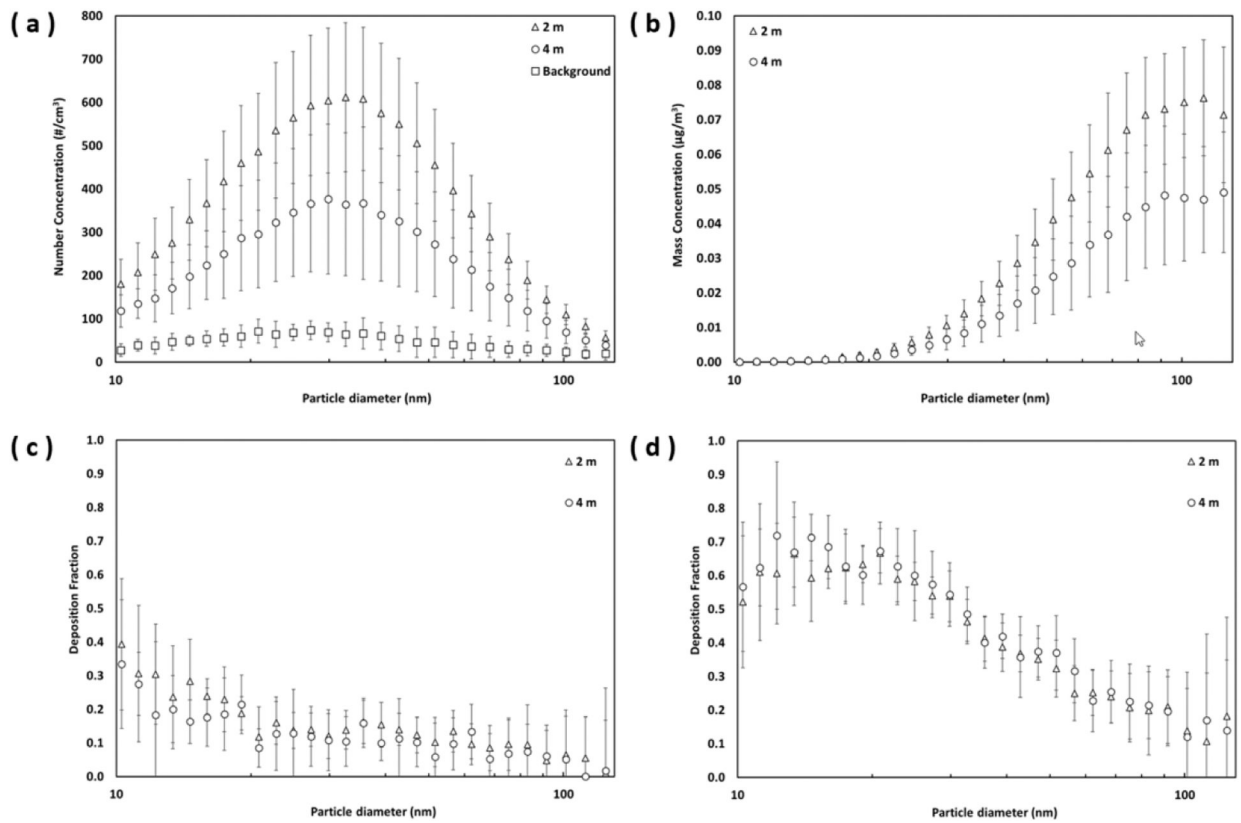The experimental set-up of e-cigarette aerosol sample collection in the laboratory.

Fig. 3.
(a) the number-based e-cigarette aerosol size distribution; (b) the mass-based e-cigarette aerosol size distribution; (c) the deposition of e-cigarette aerosol in the head-to-TB airways; and (d) the deposition of e-cigarette aerosol in the alveolar region (error bars represent one standard deviation)
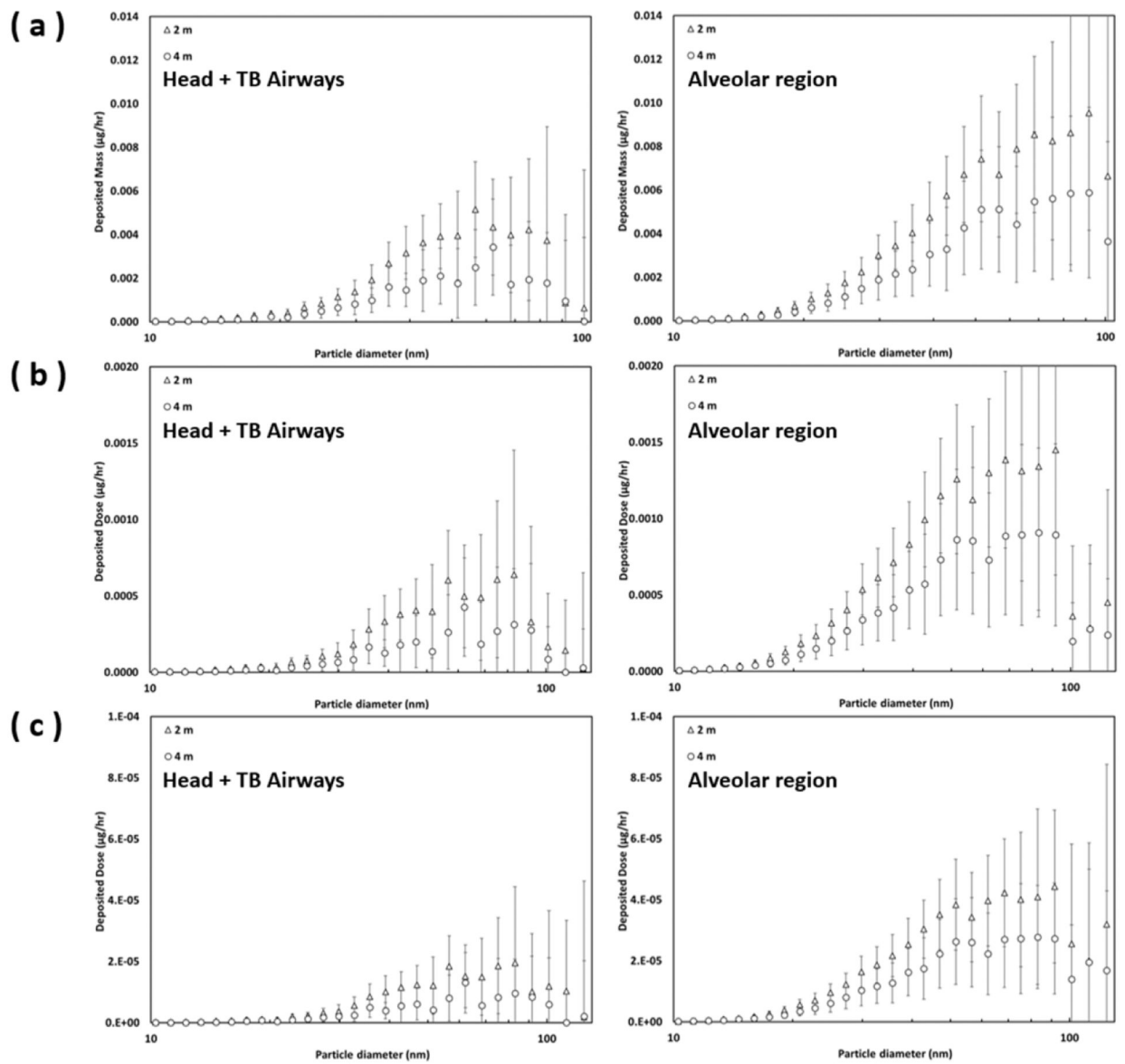
Fig. 4.
The estimated deposited dose of (a) e-cigarette aerosol, (b) Nicotine, and (c) Benzyl Alcohol in the head-to-TB airways and alveolar region by distances (error bars represent one standard deviation).
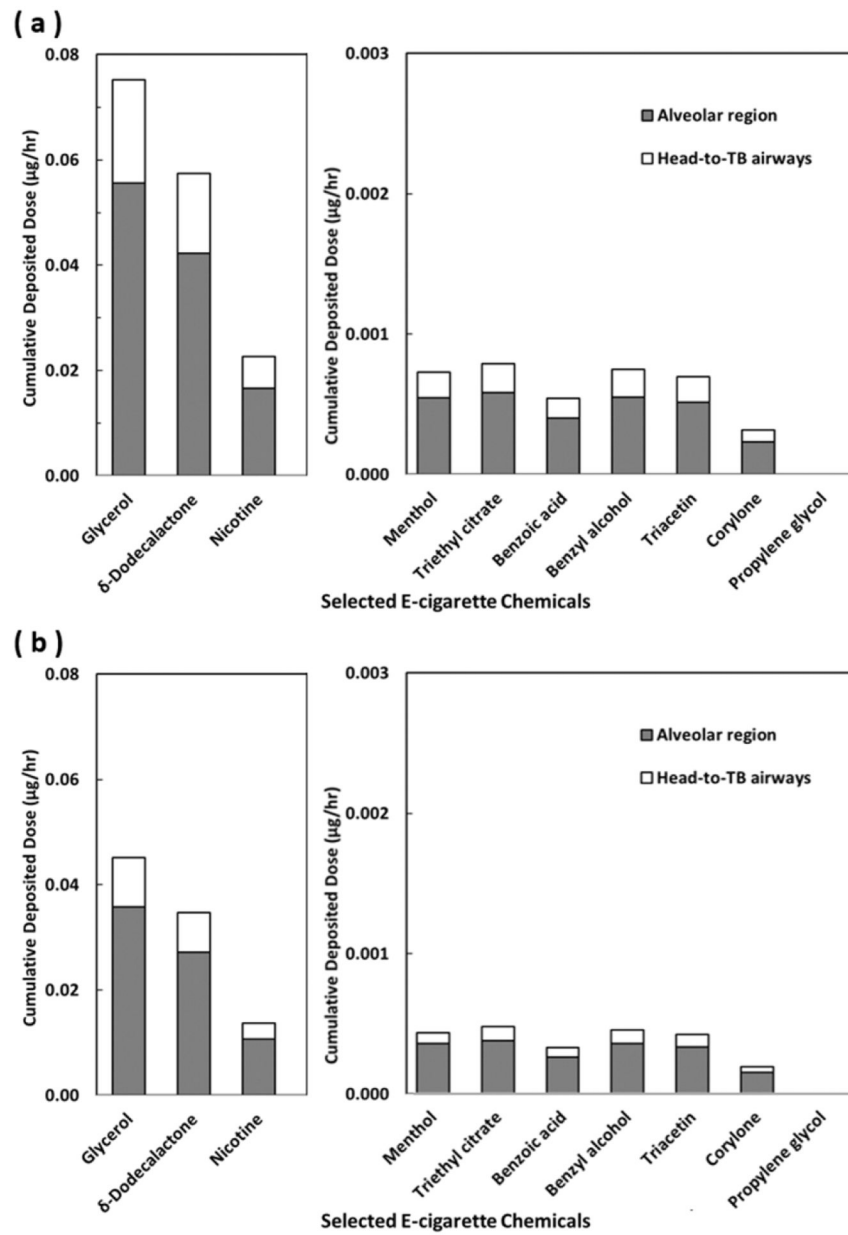
Fig. 5.
The cumulative deposited doses of selected e-cigarette chemicals in the head-to-TB airways and alveolar region for e-cigarette aerosol in 10–130 nm through passive vaping at the distance of (a) 2 m, and (b) 4 m from the active vaper.

Table 1.

The chemical constituent of size-dependent e-cigarette aerosol.

	Formula	$T_B{}^c$ (°C)	$P_v{}^d$ (mmHg)	Mass Fraction^f			
				56 d 100 (nm)	100 d 180 (nm)	180 d 320 (nm)	320 d 560 (nm)
Glycerol	$C_3H_8O_3$	290	1.68×10^{-4}	0.4356	0.6653	0.9428	0.9684
δ-Dodecalactone [*]	$C_{10}H_{18}O_2$	286	4.74×10^{-3}	0.3827	0.2376	0.0321	0.0031
Nicotine	$C_{10}H_{14}N_2$	250	3.80×10^{-2}	0.1572	0.0578	0.0028	0.0034
Menthol [*]	$C_{10}H_{20}O$	212	7.67×10^{-3}	0.0022	0.0175	0.0043	0.0003
Triethyl Citrate	$C_{12}H_{20}O_7$	294	6.87×10^{-4}	0.0048	0.0057	0.0015	0.0002
Benzoic Acid	$C_7H_6O_2$	250	7.00×10^{-4}	0.0032	0.0045	0.0129	0.0148
Benzyl Alcohol [*]	C_7H_8O	205	9.70×10^{-2}	0.0048	0.0041	0.0009	0.0002
Triacetin [*]	$C_9H_{14}O_6$	258	2.48×10^{-3}	0.0044	0.0042	0.0010	0.0001
Corylone [*]	$C_6H_8O_2$	245	4.08×10^{-2}	0.0021	0.0013	0.0012	0.0003
Propylene Glycol	$C_3H_8O_2$	188	1.30×10^{-1}	0.0000$^\$$	0.0000$^\$$	0.0000$^\$$	0.0092
Total Mass (µg)				1.51	1.55	7.16	38.7

[f] The mass of a specific chemical to the total chemical mass collected on a MOUDI stage

[c] Boiling point

[d] Reported vapor pressure at 25 °C

[*] Flavoring agent

[$] Below Detection Limit